JOURNAL OF MATERIALS SCIENCE 30 (1995) 118–126

An XPS study of the fibre–matrix interface using sized carbon fibres as a model

M. J. REIS, A. M. BOTELHO DO REGO, J. D. LOPES DA SILVA,
M. N. SOARES
Centro de Química Física Molecular, Complexo I, IST, 1096 Lisboa Codex, Portugal

This work is part of a larger project whose main objective is a better understanding of the mechanism of adhesion between the surface of carbon fibres and resins in composites. The effect over the surface of commercial PAN-based carbon fibres (Courtaulds IM CG43-750) induced by several degrees of a commercial wet oxidative surface treatment (STL) as well as the nature of the fibre–size interface have been studied by X-ray photoelectron spectroscopy. As far as functional groups are concerned, a good qualitative and quantitative characterization of the fibre surface has been achieved, using a criterium based on the requirement of internal consistency between results obtained with photoelectrons from C 1s, O 1s and N 1s peaks. Oxidative treatment induces an enrichment in oxygen and nitrogen at the surface; the presence of the former on the surface is due to the treatment but strong evidence for a residual origin of nitrogen is obtained. Coating of the commercial fibres by a prepolymer similar to the resin used as the matrix, has been used to test the type of bonding between fibre and resin before curing. Evidence is given supporting the idea that the coating (size) does not entirely cover the surface of the fibre and that only a part of it is covalently bound, alcohol groups seeming to play an important role in the adhesion mechanism.

1. Introduction

Composite materials consisting of polymeric resin reinforced by carbon fibres, especially PAN-based, have been the object of extensive research during the last few years (see [1] for a review). The aim of all of these works was to relate the mechanical performance of these materials to chemical surface fibre composition, in order to obtain a better understanding of the adhesion process between coated treated fibre and the matrix (epoxide resin).

In fact, mechanical properties of composite materials depend on adhesion between fibre and resin. Oxidative surface treatment improves adhesion; three hypotheses may be put forward to explain this improvement [2]: (1) chemical reaction between fibre and resin; (2) physical bonding (Van der Waals and hydrogen bonding); (3) mechanical interlocking; the first two mechanisms are dependent on the nature of the functional groups at the fibre surface.

On the other hand, it is known that coating (or sizing) the fibres improves the wetting of the fibre by the matrix, and protects fibre-surface reactivity [3]. The material used in this coating ("size") is matrix-compatible – an epoxide resin similar to that of the matrix but with a shorter chain – and does not contain nitrogen.

Among several techniques for chemical surface characterization, namely spectroscopic ones, X-ray photoelectron spectroscopy (XPS) is nowadays considered one of the most powerful and reliable methods to elucidate the structure, bonding and reactivity of polymeric material surfaces.

Notwithstanding the fact that charging effects, polymer degradation and serious difficulties in the curve fitting of the peaks to obtain meaningful components and internal consistency of quantitative data are responsible for the conflicting results found in the literature, the large number of contributed papers and the numerous reviews on this subject attest the great potentialities of this technique in the study of the surfaces of PAN-based carbon fibres [4–7].

Most of these studies are qualitative; quantitative analysis is restricted to the oxygen-containing functional groups formed by surface oxidation on carbon fibres. Only a small number of papers refer to the presence of nitrogen and interpret the N 1s region [8–10]. Controversial opinions still exist about its origin [5, 11]: residual, atmospheric or from the oxidative treatment.

This work on unsized and sized treated fibres not only tries to clarify this question but also uses elemental nitrogen as a probe to characterize the fibre–size interface.

2. Experimental procedure

Experiments were performed on commercial IM carbon fibres (Courtaulds IM CG43-750 tensile strength/modulus 5.5 GPa/300 GPa), the last step of the fibre production being a wet oxidative surface treatment commercially confidential. This improves wetting and bond strength between fibre and matrix. The fibres, in the present work have been commercially surface treated to different levels (STL), namely

0022-2461

STL = 0%, 10%, 50% and 100%. 0% is the untreated one and 100% the full commercial treatment.

This set of fibres has been analysed in three different situations: uncoated (unsized), coated with a short-chain epoxy resin (sized) and coated and washed with methylethylketone (washed), a good solvent for the coating resin.

The following washing conditions, with manual stirring, have been used: a few seconds, 5, 10 and 15 min in a portion of fresh solvent; 10 min in fresh solvent followed by 10 min in another portion of fresh solvent. The results in all of these conditions were identical, showing a fast removal of size by the solvent.

Samples were analysed by X-ray photoelectron spectroscopy (XPS) using a XSAM 800 (Kratos) X-ray photoelectron spectrometer operated in the FAT mode with the non-monochromatized magnesium X-radiation ($h\nu = 1253.7$ eV). The base pressure in the sample chamber was in the range of 10^{-7} Pa.

Fibre samples were mounted in a bundle arrangement such that no part of the sample holder could be detected during data acquisition. Fibres were positioned within the chamber, perpendicular to the axis of rotation of the sample holder, in order to obtain information about concentration profiles. All sample transfers were made in air.

All fibres were analysed at room temperature without further treatment. The 100% STL unsized fibre was also analysed after being water boiled for 30 min and air dried at 130 °C and kept under ultra-high vacuum for 2 months (owing to a break down of the XPS acquisition system). After a first run under these conditions, the fibre was further heated to 250 °C for 30 min and analysed once more. These last two tests were performed to check the origin of nitrogen at the surface.

Films of size, spread on to copper from an emulsion in water, have shown an irreversible degradation under X-ray irradiation (Fig. 1). This fact forced us to acquire spectra for short periods. It would be very awkward if the same problem existed with sized fibres because a good statistic for the N 1s peak requires long acquisition times. Fortunately, spectra of sized fibres are very reproducible at least during the first 12 h irradiation (Fig. 2).

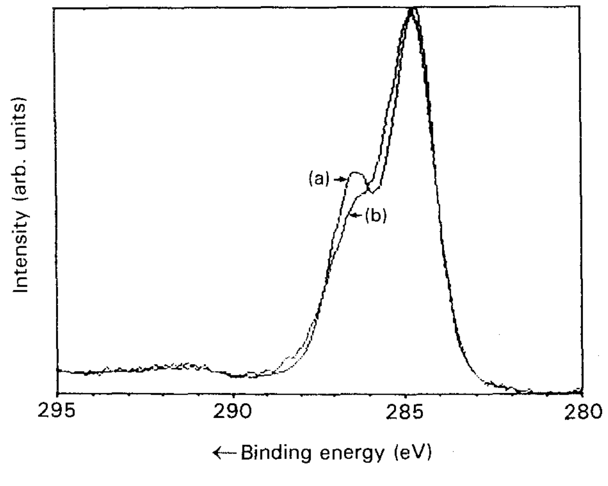

Figure 1 XPS spectra of the C 1s region for the size film spread on a copper substrate: (a) freshly introduced in the irradiation chamber; (b) irradiated for 2.5 h.

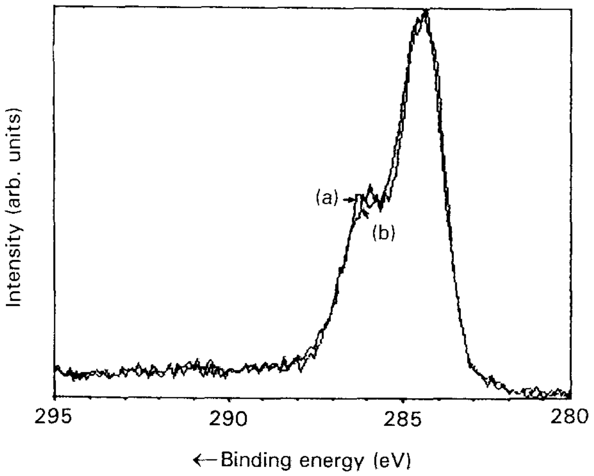

Figure 2 XPS spectra of the C 1s region for the sized 100% STL fibre: (a) freshly introduced into the irradiation chamber; (b) irradiated for 2.5 h.

Spectra were collected and stored on 200 channels with a step of 0.1 eV using a PDP-11/73 microcomputer from Digital Equipment Co. The curve fitting was carried out with a non-linear least-squares algorithm using a mixed Gaussian–Lorentzian shape, 85% gaussian (here referred to as GL85) for component peaks. For quantitative purposes, the quantification factors included in the software provided by Kratos were used.

3. Results and discussion

3.1. Unsized fibres

Overall XPS spectra are not shown for any of the samples; they are all similar, showing a strong C 1s peak, an O 1s peak and a very weak N 1s signal. All spectra were run in identical conditions, taking into account a statistical improvement of the N 1s region, but for sized fibres shorter acquisition times were used. Quantification results (in molar per cent) are summarized in Table I.

In order to understand the interaction between fibre and coating, a good characterization of the unsized fibres is needed. So, in the following, regions of the spectra concerning the C 1s, O 1s and N 1s photoelectrons will be analysed in detail, keeping in mind that information from each region should be consistent with the set.

3.1.1. C 1s region

Fig. 3 displays the C 1s peak for the 0% and 100% STL unsized fibres and for highly oriented pyrolytic graphite (HOPG). The mainly graphitic peak at 284.4 ± 0.1 eV and the $\pi \rightarrow \pi^*$ transition at 290.2 ± 0.3 eV (expanded in the insert in Fig. 3) are obvious in the fibre spectrum. This transition, characteristic of a graphitic structure, almost disappears in treated unsized fibres.

Simultaneously, the oxidized components and the aliphatic one (285.0 ± 0.1 eV) increase, the C 1s peak

TABLE I Global amounts (molar per cent) of carbon, oxygen and nitrogen and the ratio oxygen/carbon in unsized, sized and washed fibres

	Unsized fibres				Sized fibres				Size	Washed fibres			
	0%	10%	50%	100%	0%	10%	50%	100%		0%	10%	50%	100%
Carbon	95.7 ± 0.4	91.7 ± 0.5	84.4 ± 0.6	80.0 ± 0.7	84.7 ± 0.5	82.0 ± 0.5	81.4 ± 0.5	81.3 ± 0.5	80.6 ± 0.5	93.1 ± 0.5	90.3 ± 0.5	82.7 ± 0.5	79.2 ± 0.5
Oxygen	3.0 ± 0.1	6.9 ± 0.1	10.6 ± 0.1	14.1 ± 0.1	14.4 ± 0.1	17.3 ± 0.1	17.8 ± 0.1	17.3 ± 0.1	19.4 ± 0.1	6.2 ± 0.1	8.4 ± 0.1	13.8 ± 0.1	16.8 ± 0.1
Nitrogen	1.35 ± 0.03	1.40 ± 0.06	4.99 ± 0.04	5.90 ± 0.04	0.88 ± 0.05	0.61 ± 0.05	1.16 ± 0.05	1.37 ± 0.05	–	0.79 ± 0.05	1.30 ± 0.05	3.55 ± 0.05	4.02 ± 0.05
O/C ratio	0.031	0.075	0.126	0.176	0.169	0.211	0.219	0.213	0.24	0.066	0.093	0.167	0.211

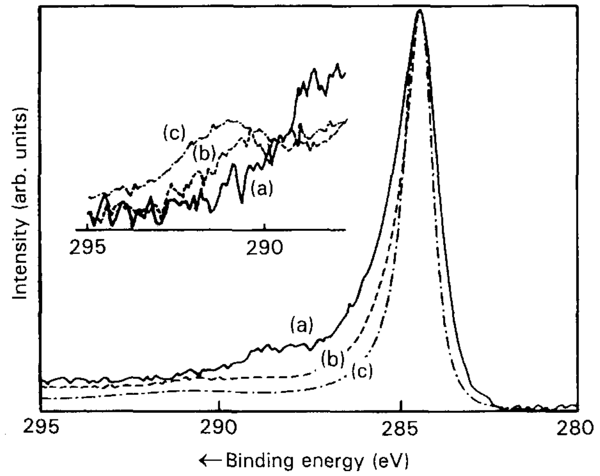

Figure 3 C 1s peak for unsized fibres compared with highly oriented pyrolitic graphite: (a) 100% STL unsized fibre; (b) 0% STL unsized fibre; (c) HOPG. In the insert, an expansion of the π → π* transition region, renormalized to the same base-line, is shown.

becoming wider. This behaviour is enhanced in the 50% and 100% STL fibres.

Curve fitting of the C 1s peak presented some difficulties of interpretation and quantification. In fact, the aliphatic and the intermediate peak, assignable to alcohol group and some nitrogen-containing functionalities, appearing at the tail of the main peak, may induce erroneous conclusions. Carboxylic functionality is the easiest to quantify, as it is characterized by higher and distinct binding energy.

All of the C 1s XPS spectra for unsized fibres were curve fitted with six peaks [10], three of them corresponding to oxidized components in the range 286–289 eV. Table II summarizes the binding energies and assignment of the components in the C 1s peak for unsized fibres, namely the alcohol, carbonyl and carboxyl groups, the aliphatic and the graphitic peaks and the π → π* transition as well as the molar per cent of the oxidized components.

As there is a superposition of chemical shifts for oxygen- and nitrogen-containing groups, both alcoholic (and ether) and amine and pyridine-type groups were included in C_3; also, both carbonyl and nitrile, imide and amino-acid groups were included in C_4.

Fig. 4 illustrates the curve fitting of the C 1s peak in six components, having a GL85 profile, for a 100% STL fibre; the insert shows the oxidized components as well as the π → π* transition peak. These results reflect a degraphitization beyond the 10% STL, a pronounced increase of the more oxidized groups (BE = 288.5 ± 0.1) with the STL and the presence of two types of carbon having intermediate binding energies, BE = 286.0 ± 0.1 and BE = 287.1 ± 0.1, assignable, respectively, to alcohols or ethers and carbonyl groups and other functional groups containing nitrogen, as summarized in Table II.

A major problem in XPS, as in other spectroscopic techniques, is curve fitting; in general cases, a photoelectron line is composed of several peaks corresponding to several chemical shifts induced by the neighbourhood of the element emitting that photoelectron line. Each peak requires at least three parameters if its

TABLE II Binding energies and assignment of the components of the C 1s peak and molar percentages of the oxidized ones (for 100% fibre) for all the unsized fibres analysed

	BE (eV)	Functional groups	Molar %			
			0%	10%	50%	100%
C_1	284.4 ± 0.1	Graphitic carbon				
C_2	285.0 ± 0.1	Aliphatic carbon				
C_3	286.0 ± 0.1	"alcohol" group COH; COC; CNH_2; > NH; 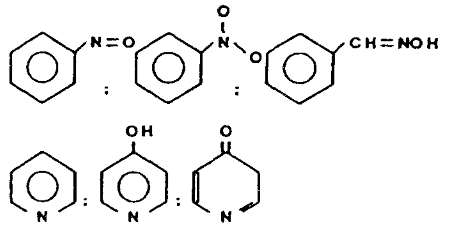	0.77	1.38	2.33	3.19
C_4	287.1 ± 0.1	("carbonyl" group) $-C{\equiv}N$; > C =N–H; C =O; $CONH_2$; CNH_2COOH	1.52	1.82	5.17	5.62
C_5	288.5 ± 0.1	(carboxylic group) COOH; COOC	1.21	2.59	4.12	5.25
C_6	290.1 ± 0.3	$\pi \rightarrow \pi^*$ transition				

profile is a pure lorentzian or gaussian (maximum intensity, FWHM and energy position); the first shape is justified by the physics of the process and the second one by the instrumental response (which usually superimposes the physical response); however, usually, a mixture of both (sum or product) is used. If, in addition, we take into account the existence of some asymmetry and tails in the peak, we can reach seven parameters for defining each one. Then, in a system such as the surface of a carbon fibre where, in the C 1s line, several chemical shifts (corresponding to different hybridizations in the carbon, different structural arrangements and different functionalities) can coexist, the problem of curve fitting would be insoluble.

Therefore, a number of constraints is necessary to extract some quantitative information from data. In this work, energy positions for each functionality have been constrained (not fixed) and the proportion of gaussian/lorentzian contents kept constant. Furthermore, an iterative method based on the assumption that an internal consistency should be obeyed, has been followed: taking into account that some carbon is bound to nitrogen, the sum of molar per cent of O 1s and N 1s peaks should be equal to the molar per cent of the "oxidized" carbon area ($C_3 + C_4 + 2C_5$), the multiplying factor for C_5 arising from the stoichiometry in carboxylic acids (O:C = 2:1). The molar per cent have been computed using quantification factors provided by apparatus software and including relative cross-sections, relative escape depths and an apparatus response function.

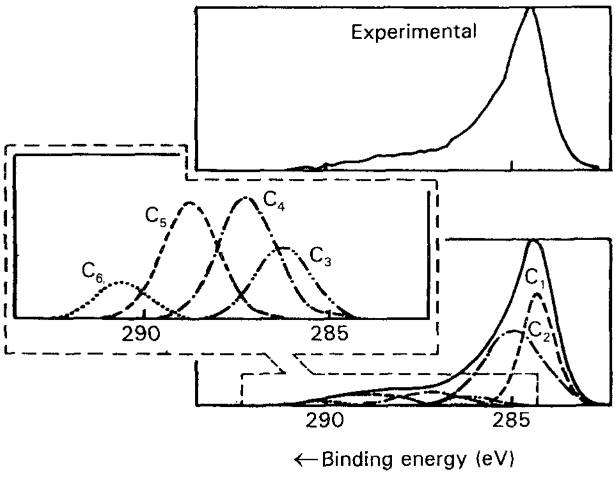

Figure 4 C 1s peak fitting with six gaussian–lorentzian components for the 100% STL unsized fibre: C_1, graphitic carbon; C_2, aliphatic carbon; C_3, alcohol and amine groups; C_4, carbonyl, amide, amino-acids, nitroso, etc. (see Table II for a more exhaustive listing); C_5, carboxylic groups; C_6, $\pi \rightarrow \pi^*$ transition.

Being aware of the fact that this internal consistency could be hidden by the existence of concentration profiles (due to the differences in escape depths, λ, for C 1s, N 1s and O 1s photoelectrons), we tested, for several schematic concentration profiles, the relative error in computing the molar per cent of a given oxidized group using the carbon peak alone, or using the O 1s and N 1s peaks. A maximum relative error of 8% was obtained for oxygen-containing functions (we took, for our calculations, $\lambda_O \approx 0.89\,\lambda_C$ and $\lambda_N \approx 0.95\,\lambda_C$ [12]).

3.1.2. O 1s region

Based on data from NIST Standard Reference Database [13] and recent literature [6, 10, 14, 15], all the O 1s peaks for unsized fibres were curve fitted with four peaks, justified by the presence of the carbonyl and alcohol functions and two different oxygen atoms in the carboxylic group (Table III). The variation of the components O 2 and O 4 (carboxylic group) seems to be larger than the other ones, indicating a preferential formation of this functional group by STL, at least at the surface.

For further clarifying this question, we made angular measurements changing the take-off angle relative

TABLE III Assignment and molar per cent (for 100% fibre) of the components of the O 1s peak for all the unsized fibres analysed

STL (%)	O_1 (C =O)		O_2 (COOH)		O_3 (COH)		O_4 (COOH)	
	BE (eV)	(%)	BE (eV)	(%)	BE (eV)	(%)	BE (eV)	(%)
0	530.9	0.10	531.6	0.91	532.2	1.04	533.3	0.94
10	530.6	0.64	531.6	2.45	532.2	1.30	533.3	2.46
50	530.9	0.86	531.5	4.11	532.2	1.55	533.2	4.10
100	530.7	0.91	531.6	5.59	532.3	2.01	533.2	5.52

to the longitudinal axis of the fibre where corrugations are not expected to be important, compared with the average thickness of oxidized overlayers.

In the 100% STL fibre, the molar per cent of oxygen decreases with the take-off angle relative to the surface, β, as shown in Fig. 5. If we assume for the oxygen a concentration profile having an analytical expression $n_O^s - x(n_O^s - n_O^b)/l_O$, x being the depth from the surface, n_O^s the molar per cent of oxygen in the first layer at the surface and l_O the depth where the molar per cent becomes n_O^b, the assumed bulk uniform concentration, we have

$$n_O^\beta = n_O^s + (n_O^s - n_O^b)\frac{\lambda_O \sin(\beta)}{l_O} \times \left\{\exp\left[-\frac{l_O}{\lambda_O \sin(\beta)}\right] - 1\right\} \quad (1)$$

λ_O being the escape length for oxygen in the medium, n_O^β the molar per cent of oxygen measured at a take-off angle, β. Experimental data for oxygen are fitted by Equation 1 if $l_O \sim 4\lambda_O$, $n_O^s \sim 12.9$ and $n_O^b \sim 1.6$.

Obviously, this concentration profile is merely schematic; the complexity of the system and the uncertainty about the surface topography does not allow a deeper analysis of this question; for the sake of simplicity, a linear profile was assumed which giyes us a rough idea of the oxygen distribution.

In a fast observation, it seems that the observed variation cannot be assigned to any functionality in particular, as shown in Fig. 6, for the O 1s and C 1s region, where we can see a general increase in the oxidized carbons with take-off angle and very similar distributions in the O 1s peak for two different take-off angles.

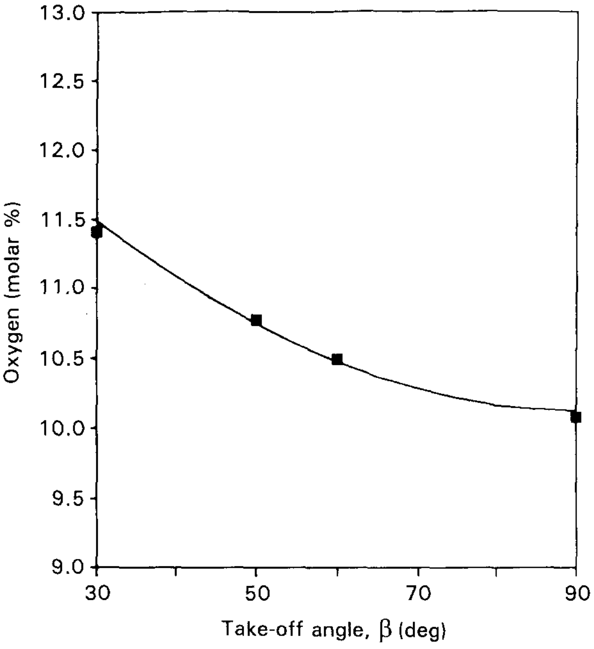

Figure 5 Angular dependence of the measured molar fraction of oxygen in a 100% STL unsized fibre. Fitted line has the analytical form of Equation 1, with $l_O/\lambda_O \sim 4$, $n_O^s \sim 12.9\%$ and $n_O^b \sim 1.6\%$.

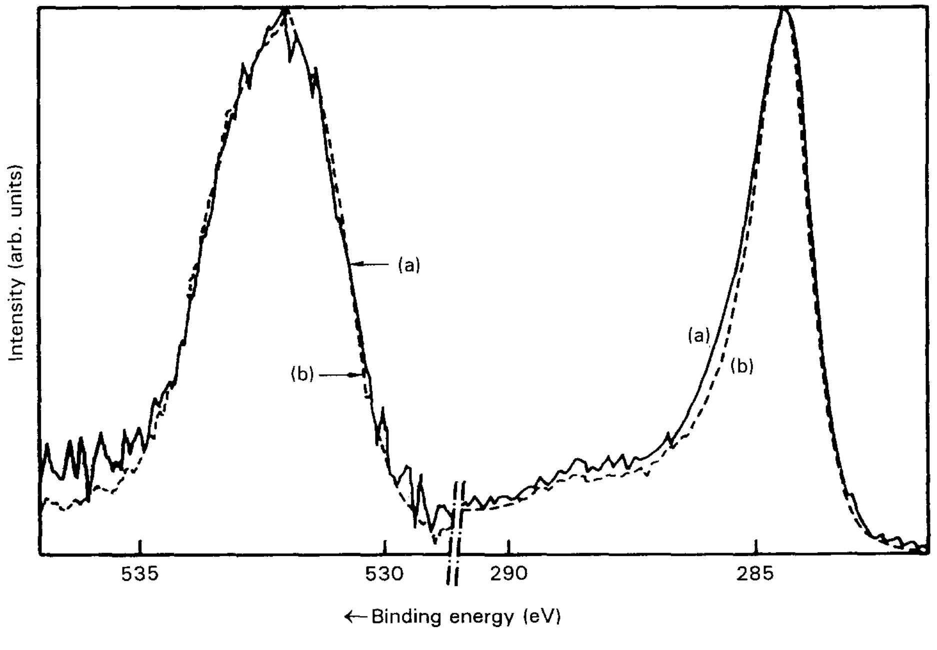

Figure 6 Comparison between the C 1s an O 1s regions for the 100% STL fibre at (a) 30° and (b) 90° take-off angle.

However, the difference between C 1s peaks for two extreme take-off angles relative to the surface (30 ° and 90 °) may induce the idea of a more important increase for the alcohol group at the surface than for the carboxylic group. As these variations are very slight and there is a large superposition of peaks around the binding energy corresponding to the alcohol group, it is not possible to make a quantitative demonstration of this assessment.

3.1.3. N 1s region

In most recent works, the N 1s data have not been considered or, when presented, were not analysed in terms of nitrogen-containing groups. This can be justified because the N 1s signal from the carbon fibre surface is much weaker than C 1s or O 1s signals. The curve fitting of N 1s spectra presents some problems owing to the poor statistics of the peak. Therefore, this has been done just for the fibres richer in nitrogen: i.e. the unsized ones. The best fitting was achieved with three peaks (BE = 398.6 ± 0.1, 399.7 ± 0.1 and 401.0 ± 0.1 eV) for 10%, 50% and 100% STL unsized fibres as shown in Fig. 7a. For the 0% STL fibre, a new peak (BE = 402.6 eV) instead of the lowest BE one (BE = 398.6) was necessary to have a good curve fitting (Fig. 7b and Table IV).

A tentative assignment of the N 1s peak components is as follows: in the surface-treated fibres, the lowest BE peak may arise from amines, imines and piperidine structures. The two higher BE peaks arise from residual nitrogen (nitrile, amides, imides, amino-acids, cyclic structures (pyridine type) having oxygenated substituent groups). The peak at 402.6 eV in the untreated fibre can be assigned to highly oxidized nitrogen compounds (nitroso and nitro compounds), probably formed during the graphitization process.

The existence of the peak at 402.6 eV, in the 0% STL fibre, together with the fact that the N 1s peaks are similar in the 50% and 100% STL fibres (both qualitatively and quantitatively), and qualitatively similar to the one in the 10% STL, is compatible with the following hypothesis. The surface treatment breaks down superficial "fringes" where nitrogen exists mainly not incorporated in cyclic structures and at a lower density than in the bulk. Therefore, for greater STL most of the detected nitrogen is residual nitrogen from PAN remaining in the bulk and therefore exhibiting a similar distribution in all treated fibres where the destruction of the "fringes" is complete. This being the case, nitrogen would appear incorporated in saturated or unsaturated cycles for higher STL.

TABLE IV Areas and binding energies for the components of the N 1s peak (for 100% fibre) for all the unsized fibres analysed

STL	N_1		N_2		N_3	
	BE (eV)	(%)	BE (eV)	(%)	BE (eV)	(%)
0%	–	–	399.6	0.69	401.0	0.55
10%	398.5	0.15	399.7	0.96	401.0	0.24
50%	398.7	0.92	399.8	3.04	401.0	1.05
100%	398.7	0.82	399.8	3.65	401.1	1.39

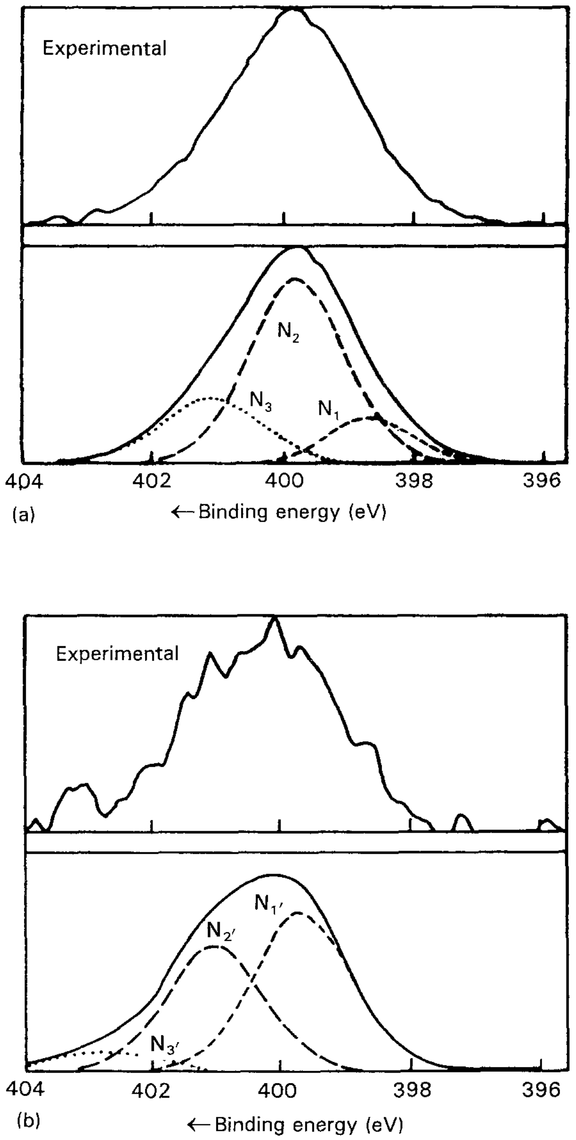

Figure 7 N 1s peak fitting with three gaussian–lorentzian components: (a) for the 100% STL unsized fibre: N_1, amines and imines (BE = 398.6 ± 1 eV); N_2, amides, imides, pyridines and nitriles (BE = 399.7 ± 0.1 eV); N_3, oximes and oxazoles (BE = 401.0 ± 0.1 eV); (b) for the 0% STL unsized fibre: $N_{1'}$, amides and nitriles (BE = 399.6 eV); $N_{2'}$, amino acids (BE = 401.0 eV); $N_{3'}$, nitro and nitroso compounds (BE = 402.6 eV).

In the untreated fibre, the "fringes" were not yet destroyed. For this reason the amount of nitrogen present at the surface is lower than in the highly treated surfaces and a small amount can be assigned to highly oxidized nitrogen compounds resulting from the carbon fibre production process itself.

The hypothesis of nitrogen being put on the surface by the oxidative bath has been tested by repeating spectra over one of the fibres, the 100% STL, after being water boiled for 30 min and air dried at 130 °C and kept under ultra-high vacuum (UHV) for 2 months. No qualitative or quantitative changes in the nitrogen, oxygen and carbon peaks were noticed. Another spectrum was run after heating the same fibre, under UHV, to 250 °C for 30 min and, once more, no modifications were noticed.

To clarify this aspect further, nitrogen fractions have been measured as a function of take-off angle, β,

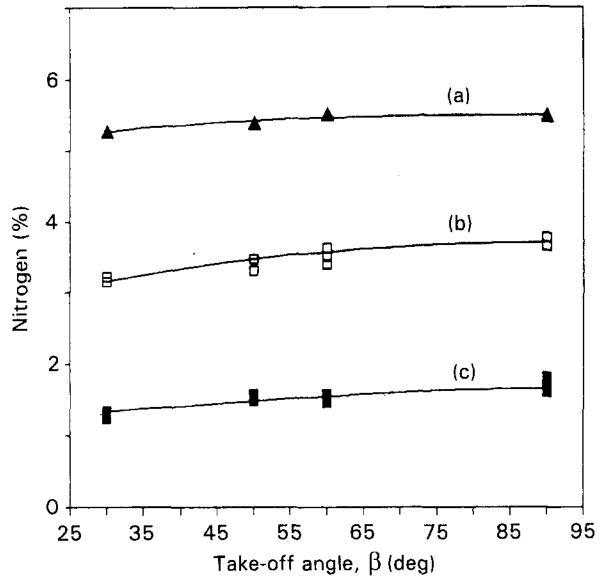

Figure 8 Angular dependence of the measured molar per cent of nitrogen in 100% STL fibres: (a) unsized, (b) washed, and (c) sized. Fitted curves in (b) and (c) obey a law given by Equation 6, s having, respectively, the values $1.5\lambda_N$ and $2.7\lambda_N$.

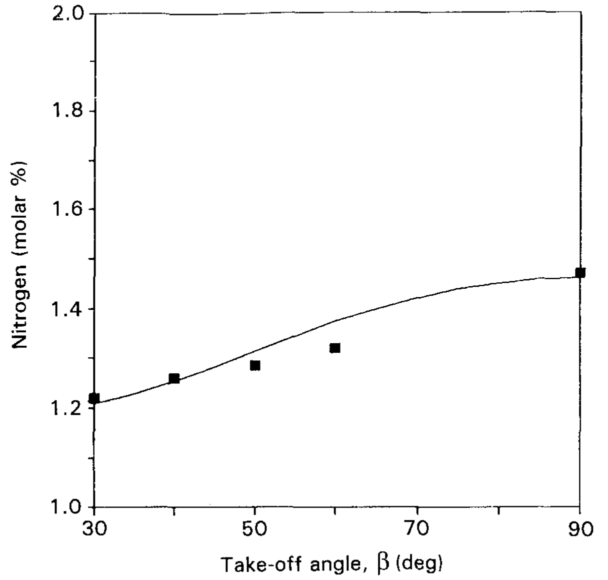

Figure 9 Angular dependence of the measured molar fraction of nitrogen in a 10% STL unsized fibre. The fitted line has the analytical form of Equation 3 with $n_N^b \sim 5.8\%$, $n_N^s \sim 1.4\%$, $l_1/\lambda_N \sim 0.73$ and $l_2/\lambda_N \sim 5.5$.

in 100% and 10% STL fibres. Both show a variation with β (Figs 8a and 9). As for the oxygen profile, we used linear schematic profiles displayed in Fig. 10, which give for measured molar per cent, n_N^β, the analytical Equations 2 and 3 for profile 1 (100% STL fibre) and profile 2 (10% STL fibre), respectively

$$n_N^\beta = n_N^b \frac{\lambda_N \sin(\beta)}{l_N}\left\{1 - \exp\left[-\frac{l_N}{\lambda_N \sin(\beta)}\right]\right\} \qquad (2)$$

$$n_N^\beta = \frac{n_N^b \lambda_N \sin(\beta)}{l_2}\left\{1 - \exp\left[-\frac{l_2}{\lambda_N \sin(\beta)}\right]\right\} - \frac{n_N^s \lambda_N \sin(\beta)}{l_1}\left\{1 - \exp\left[-\frac{l_1}{\lambda_N \sin(\beta)}\right] - \frac{l_1}{\lambda_N \sin(\beta)}\right\} \qquad (3)$$

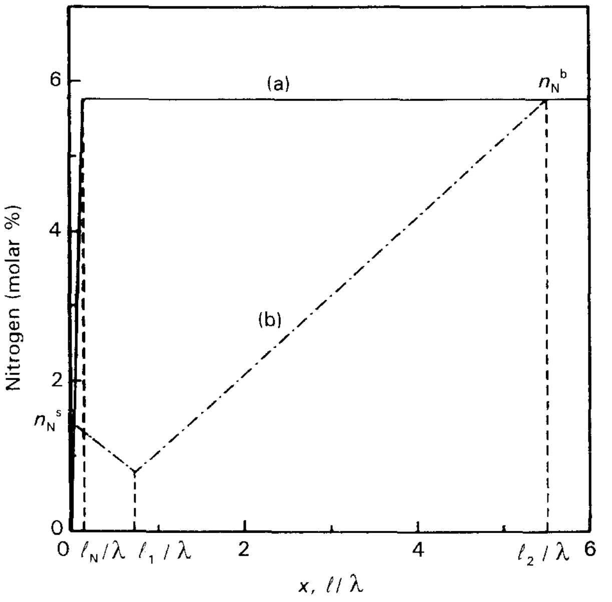

Figure 10 Nitrogen profiles: (a) 100% STL unsized fibre; (b) 10% unsized fibre.

n_N^b being the assumed bulk molar per cent, λ_N the escape length for photoelectrons from nitrogen in the medium and l_N, l_1 and l_2 the depths defined in Fig. 10.

The best parameters are also shown in the Fig. 10 and it is interesting to note that the bulk composition obtained with 10% and 100% STL fibres is the same and that the gradient extends over a much larger region in the less treated fibre (10% STL), which supports our hypothesis about the origin of nitrogen and the action of the treatment.

Parameters obtained for the 10% STL fibre give a V-shaped profile for nitrogen molar per cent; this schematic shape may be related to the escape mechanism of nitrogen during the graphitization process, because with 10% STL only a part of the fringes must have been cut.

3.2. Sized fibres

In the spectra of sized fibres (washed or not), a N 1s peak is observed. In washed fibres the N 1s peak intensity is intermediate between the sized and unsized fibre with the same STL. As the sizing compound is an epoxy resin (therefore, it does not contain any nitrogen), we can conclude that either the thickness of the size is less than the analysis depth in XPS or the size film has some holes (or has a sort of island-like structure).

If the first hypothesis holds, the ratio between the intensity of the N 1s peak in sized or washed fibres and the intensity in the unsized fibre is related to the average thickness of the film.

In fact, assuming a uniform density along fibre and size, similar densities for fibre and size and similar escape depths, λ_N, in both media, we can write

$$n_N(\text{sized fibre}) = n_N(\text{unsized fibre})\exp(-s/\lambda_N) \qquad (4)$$

s being the assumed uniform thickness of size layer and n_N the molar per cent of nitrogen under the size film.

In this case, the intensity of the N 1s peak in the sized or washed fibres should change with the take-off angle, β, in the following way

$$n_N^\beta(\text{sized fibre}) = n_N^\beta(\text{unsized fibre}) \times \exp[-s/\lambda_N \sin(\beta)] \quad (5)$$

For the second hypothesis – island-like structure for the size film – and assuming a film thickness negligible compared with the hole dimensions (in order to have negligible "shadow" effects), we will have

$$n_N^\beta(\text{sized fibre}) = n_N^\beta(\text{fibre})\,\{(1-f) + f\exp[-s/(\lambda_N \sin\beta)]\} \quad (6)$$

f being the fraction of fibre surface covered by the size, and $1-f$ the uncovered fraction.

Only 100% STL fibre has been tested, because its nitrogen content is the largest one, allowing sounder quantifications. Both for sized and washed fibres a change in the intensity of the N 1s peak with angle has been measured. However, that variation is not consistent except with Equation 6, as displayed in Fig. 8b and c. Computed values of f, for best fittings, were 0.75 and 0.42 for sized and washed fibres, respectively, while s, the average size thickness, was about 2.7 λ_N and 1.5 λ_N.

From these values we can conclude that (a) the size does not completely cover the fibre surface, (b) the size is not completely bound by covalent bonds; it is, at least partly, bound by intermolecular bonds (dipolar and/or hydrogen bond type) otherwise it would not be removed by a solvent. On the other hand, covalent bonding between size and nitrogen is not very plausible because this should modify its functional distribution, which is not observed.

Spectra of sized fibres, washed or not, in the C 1s region, are different from spectra both of the "size" and the unsized fibres. Compared with spectra from unsized fibres with identical STL, sized fibres show a large decrease of the peak corresponding to carboxylic groups (BE = 288.5 ± 0.1) and an increase of the intensity in the region centred at 286.5 eV. Washed fibres show an intermediate behaviour (Fig. 11).

The partial disappearance of carboxylic groups can be interpreted in two ways: (1) they have been covered by size film; (2) they have reacted with size molecules. This last hypothesis is not very likely because even if there is a reaction, its product still contains carboxylic groups (it changes from acid to ester function). Therefore, only the first hypothesis can explain the large decrease of carboxylic intensity. So, this group could be used, as can nitrogen, as a probe to estimate the thickness of the size film because it is not present in the size.

In Fig. 12 a plot of angular variations of intensity for carboxylic groups in unsized, washed and sized fibres are shown. Lines were obtained, assuming for the carboxylic group a concentration profile identical with the one found for oxygen in the unsized fibre; in the case of washed and sized fibres the structure and thickness assumed for the size were identical with that obtained from the nitrogen. In all of them the best coincidence with experimental points was obtained assuming that the carboxylic group contains 60% of the total oxygen, and this has been the only free parameter; for all the others, n_O^s, n_O^b, l_O/λ_O, f and s/λ_O, the values obtained from the angular analysis of the oxygen in unsized fibres and of the nitrogen in sized and unsized fibres were kept unchanged. This fact, associated with the previous observation that the top surface seemed to be enriched in alcoholic groups when compared with the inner layers, suggests, as the most probable reaction between the fibre and the resin, the one involving the alcoholic groups at the surface.

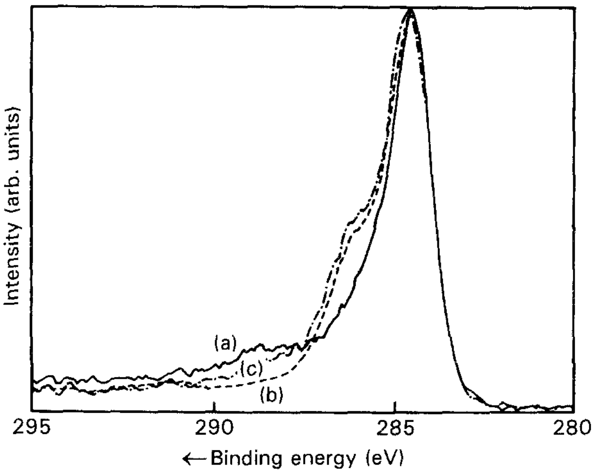

Figure 11 Comparison between C 1s peaks of 100% STL fibres: (a) unsized; (b) sized; (c) washed.

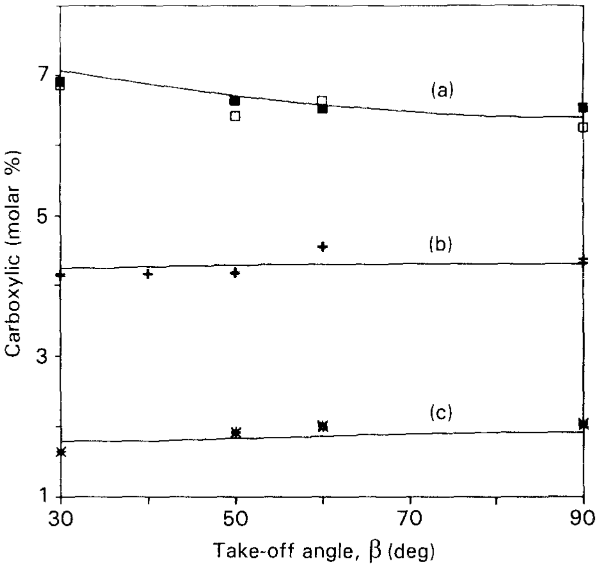

Figure 12 Angular dependence of the measured carboxylic molar per cent in 100% STL fibres: (a) unsized; (b) sized; (c) washed. Experimental points were obtained by curve fitting of the C 1s peak, except empty squares in the unsized fibre, which were obtained by curve fitting of the O 1s peak.

4. Conclusion

XPS results on unsized treated fibres point to an increase of the oxidized functions at the surface induced by the oxidative surface treatment and strongly suggest a residual origin for nitrogen, as well as an effect of the STL consisting in the cut of fringes from the fibre surface.

XPS angular distribution data associated with schematic concentration profiles show the existence of concentration gradients: an enrichment in oxygen at the surface, as expected, and a superficial depletion of nitrogen, especially in the 10% STL fibre, reinforcing the preceding hypothesis about both the nitrogen origin and the oxidative treatment action over the surface.

Usually, after the oxidative treatment, the fibre is coated by the size which has the same composition as the polymeric matrix. Because, contrary to the fibre, the size does not contain nitrogen, the variation of the intensity of N 1s photoelectrons as a function of take-off angle was used as a probe for testing the structure and thickness of the size. The obtained results revealed that the size does not completely cover the fibre and the washing operation removes a fraction of it, thus decreasing the average thickness of the size remaining. Therefore, it seems reasonable to assume that the size is bound covalently and in an intermolecular way.

The qualitative and quantitative behaviour of the carboxylic groups in the sized and washed fibres were very similar to nitrogen. Using the carboxylic group as a probe, the values of the covered fibre fraction estimated using these data agree, within experimental error limits, with those previously obtained with nitrogen, showing that the size does not preferentially bind to the carboxylic group, contrary to what is usually assumed. This reinforces the hypothesis of Sherwood and co-workers [14, 15] that the chemical reaction between the epoxidic group of the resin and the fibre surface, yielding covalent bonding, may occur mainly through the alcoholic group at the surface.

Acknowledgements

The authors thank the European Commission for the financial support and the partners in the EURAM-programme Contract no. MA1E/0047/C (Department of Materials, University of Surrey, Katholieke Universiteit Leuven, ICI Advanced Materials and DLR) for their participation in the fruitful discussions, especially Dr Muriel Desaeger. The authors are also grateful to the JNICT and INIC for their financial aid.

References

1. E. FITZER, in "Carbon Fibers Filaments and Composites", Series E, "Applied Sciences", edited by J. L. Figueiredo, C. A. Bernardo, R. T. K. Baker and K. J. Hüttinger, Vol. 177, (Dordrecht, 1990) pp 3, 169.
2. B. RAND and R. ROBINSON, *Carbon* **15** (1977) 257.
3. E. FITZER and R. WEISS, *ibid.* **25** (1987) 455.
4. F. HOPFGARTEN, *Fibre Sci. Technol.* **12** (1979) 295.
5. K. WALTERSSON, *ibid.* **17** (1982) 289.
6. Y. NAKAYAMA, F. SOEDA and A. ISHITANI, *Carbon* **28** (1990) 21.
7. A. ISHITANI, in "Molecular Characterization of Composite Surfaces", edited by H. Ishida and G. Kumar, Proceedings of the Symposium on Polymer Composites: Interfaces, (New York, 1985) p. 321.
8. C. KOZLOWSKI and P. M. A. SHERWOOD, *Carbon* **24** (1986) 357.
9. Y. XIE and P. M. A. SHERWOOD, *Chem. Mater.* **2** (1990) 3.
10. E. DESIMONI, G. I. CASELLA, A. M. SALVI, T. CATALDI and A. MORONE, *Carbon* **30** (1992) 527.
11. C. LEFEBVRE, J. VERBIST, D. LEONARD and P. BERTRAND, in "Polymer–Solid Interfaces", edited by J. J. Pireaux, P. Bertrand and J. L. Brédas, Proceedings of the 1st International Conference on Polymer-Soild Interfaces, (Namur, 1992) p. 145.
12. K. WALTERSSON, *Fibre Sci. Technol.* **17** (1982) 289.
13. C. D. WAGNER, "NIST X-ray Photoelectron Spectroscopy Database", US Department of Commerce (NIST, 1989).
14. C. KOZLOWSKI and P. M. A. SHERWOOD, *Carbon* **25** (1987) 751.
15. Y. XIE and P. M. A. SHERWOOD, *Chem. Mater.* **1** (1989) 427, and references therein.

Received 8 November 1993
and accepted 16 June 1994